Q2D-morfo

A morphodynamic quasi-2DH coastline model

Version 1

A. Falqués

22nd November 2006

Applied Physics Department
Universitat Politècnica de Catalunya

1 Foreword

This is a morphodynamic model for coastline evolution at medium to long term, i.e., weeks to years. It is an extension of the traditional one-line models by considering the cross-shore coordinate up to some extent. In this sense it is in between one-line models and morphodynamic area models for the nearshore. Actually, it is an alternative approach to the existing N-line modelling. This report explains the first version of the model which allows only for moderate amplitude shoreline features.

2 Aim and rationale

In spite of the complexity of 3D nearshore morphodynamics, the so-called one-line modelling has had some success in understanding and predicting the dynamics of sandy coastlines at large space and time scales [*Pelnard-Considère*, 1956; *Horikawa*, 1988; *Komar*, 1998]. This is a severe simplification and consists in averaging on the vertical and the cross-shore directions so that the morphodynamical active region collapses in a single line which represents the coastline. The changes in coastline position are then given by convergence/divergence of the total alongshore sediment transport rate Q which is determined just by the wave forcing without account of surf zone hydrodynamics (water inertia, mass conservation, etc.). Cross-shore sediment transport is usually not explicitly considered. It is however always implicit to ensure the sediment redistribution that is necessary to reach the equilibrium beach profile after the changes which are driven by alongshore transport. Despite all those simplifications, the one-line modelling has been used for years, specially by coastal engineers and has proven to have reasonable skill for coastline evolution prediction at large time and space scales (years and km's) [*Larson et al.*, 1987; *Larson and Kraus*, 1991].

The standard one modelling has however a number of important shortcomings. First, a stable shoreline is always predicted in contrast with the finding of *Ashton et al.* [2001] according to which the shoreline may become unstable if the wave incidence angle is large enough. Second, the governing equation for small deviations from a rectilinear shoreline is a diffusion equation. This precludes the modelling of shoreline sand wave propagation which are sometimes observed [*Inman*, 1987; *Thevenot and Kraus*, 1995; *Ruessink and Jeuken*, 2002; *Falqués*, 2002; *Falqués and Calvete.*, 2003; *Falqués*, 2005]. These two drawbacks are caused by the fact that the traditional one line modelling neglects the effect of nearshore bathymetric changes associated to changes in coastline on the wave propagation from deep water up to breaking [*Falqués and Calvete*, 2005]. In addition to exclude shoreline instability, those effects also produce a decrease of shoreline diffusivity so that the traditional

model tends to over-predict shoreline diffusivity [*Falqués*, 2003]. Finally, another limitation of the traditional one-line model as set up by *Pelnard-Considère* [1956] (see also *Larson et al.* [1987]) is its linearity, i.e., it is valid only for small departures of a rectilinear shoreline.

Falqués and Calvete [2005] have developed a linear stability model of the coastline based on the one-line concept but including the bathymetric changes associated to coastline changes in a simplified way (1D-morfo model). This model describes high angle wave shoreline instability and sand wave propagation. It has nevertheless a number of limitations:

1. The cross-shore profile dynamics which is proven to be crucial [*Falqués and Calvete*, 2005]is ignored and a fixed cross-shore shape function is considered for the bathymetric signal of the shoreline disturbances.
2. As it is a linear stability model it only allows for small amplitude departures of a rectilinear coastline.
3. Since it is based on an analysis of alongshore propagating harmonic modes on an open coast it is not straightforward how to adapt it to beaches bounded by structures.
4. The model is aimed at the free dynamic problem of the coastline and, again, the adaptation to a forced problem (e.g. propagation of sand waves along a sandy coast under the forcing by an adjacent tidal inlet dynamics, see *Falqués* [2005]) is not obvious.
5. The wave driver in 1D-morfo is fixed, simply consisting of the wavenumber irrotationality, wave energy conservation and dispersion relation.

The new Q2D-model is aimed at overcoming all these limitations. The sediment transport is considered in two dimensions on the whole nearshore, not only at the coastline as the one-line models. Also, the wave propagation on the evolving 2DH topography is considered. By these two reasons it is a 2DH model. However, the nearshore hydrodynamics is not considered because the sediment transport is based on a cross-shore distributed CERC formula and on a parameterized diffusive transport. This assumption filters out all the rich self-organized morphodynamic processes of the surf zone associated to rip currents and meandering longshore current (see, for instance, *Falqués et al.* [2000],*Caballeria et al.* [2002], *Ribas et al.* [2003] *Falqués et al.* [2005]). This is the most important limitation of the model and poses an evident lower bound to the resolved lengthscales which is in the order of the surf zone width. In this sense the new model is only Q2DH. It has however a number of important improvements. First, it lifts assumption 1) of 1D-morfo. Also,

the maximum amplitude of coastline features can be quite large so that it is not 'infinitesimal',i.e., assumption 2) is removed. The new model computes the morphodynamic development in time of the nearshore bathymetry and shoreline shape by solving the initial value problem. This overcomes both limitations 3) and 4). Finally, the wave driver can be freely chosen as it is just a subroutine of the time evolution code.

3 Formulation and basic equations

3.1 Geometry, integration domain and grid

The integration domain is inside the rectangular and horizontal domain $\{0 \leq x \leq L_x; 0 \leq y \leq L_y\}$. The y axis is chosen with an orientation similar to the mean orientation of the initial shoreline and in such a way that there is some distance between the axis and the initial shoreline. A rectangular grid is chosen, running from $i = 0$ up to $i = n$ in the direction of the x axis and from $j = 0$ up to $j = m$ in the direction of the y axis. A staggered grid is also defined, from $ic = 1$ up to $ic = n$ and from $jc = 1$ up to $jc = m$. If the grid spacings are $\Delta x = L_x/n, \Delta y = L_y/m$, the basic grid and the staggered one are defined as:

$$x(i) = i\,\Delta x \quad i = 0, 1, 2, ...n \qquad , \qquad y(j) = j\,\Delta y \quad j = 0, 1, 2, ...m \tag{1}$$

$$\begin{aligned} x(ic) &= x(i) - \Delta x/2 \quad i = ic, \quad ic = 1...n \\ y(jc) &= y(j) - \Delta y/2 \quad j = jc, \quad jc = 1...m \end{aligned} \tag{2}$$

The topography is given by $z = z_b(x, y)$ and $z = z_s$ defines the mean water level. The grid position of the shoreline is defined by $ic = ishore(jc)$ which is the smallest ic such that $D(x(ic), y(jc)) = z_s - z_b(x(ic), y(jc)) \geq 0$. By linear interpolation between $z_b(x(ic), y(jc))$ and $z_b(x(ic-1), y(jc))$ the cross-shore position $x_s(y)$ where $D(x_s(y), y) = 0$ is computed. The $x = x_s(y)$ line determines a smooth shoreline. For certain applications, the wave set-up can be incorporated. This may be done by computing the total approximated set-up at the shoreline $z_{su} = 0.15H_b$ (see *Short* [1999], pag. 79) and then making

$$D(x, y) = z_s - z_b(x, y) + \frac{z_{su}(y)}{X_b(y)}(x_s(y) + X_b(y) - x) \tag{3}$$

whenever $x < x_s(y) + X_b(y)$ instead of that expression for $D(x, y)$.

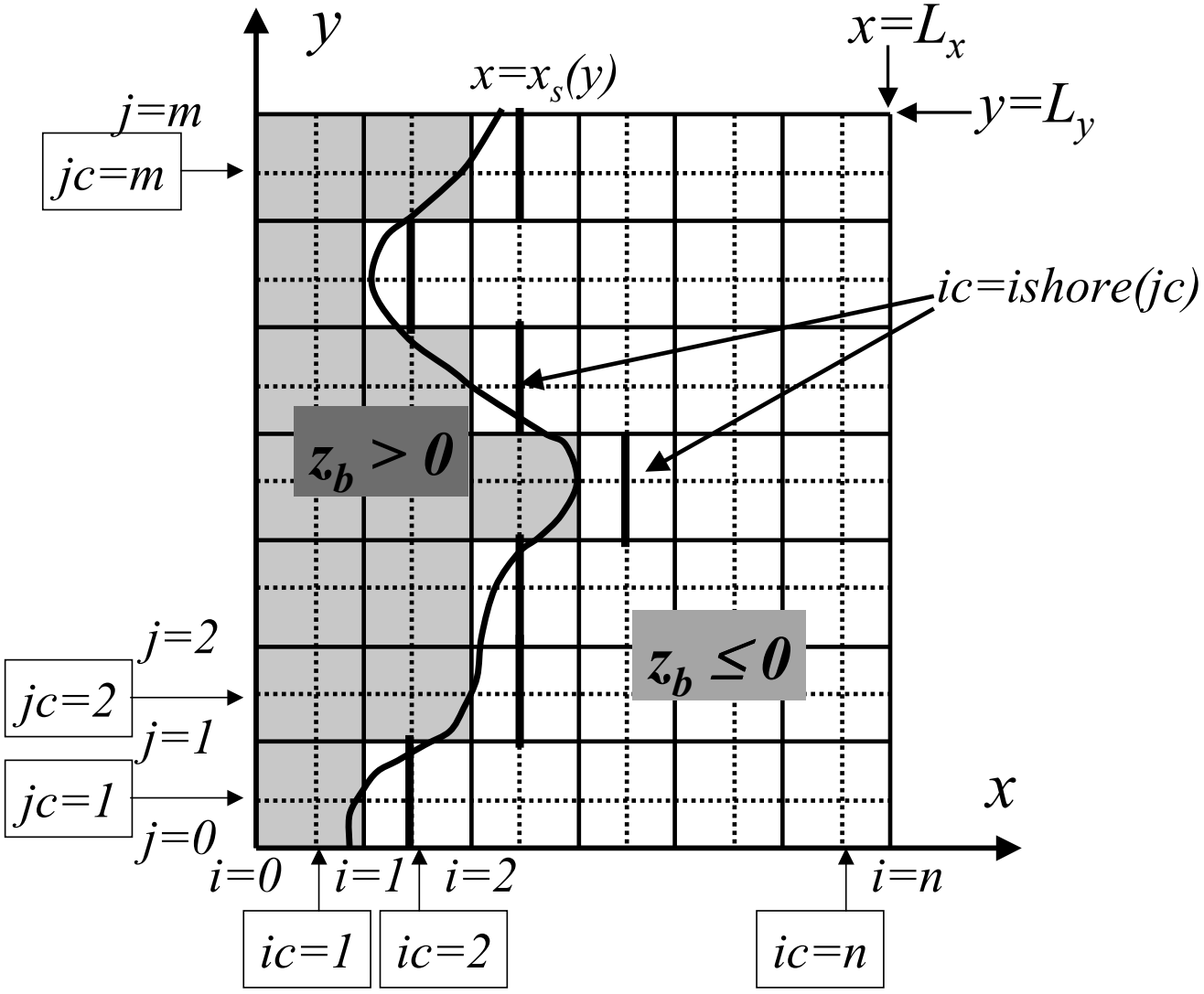

Figure 1: Geometry of the domain and integration grid.

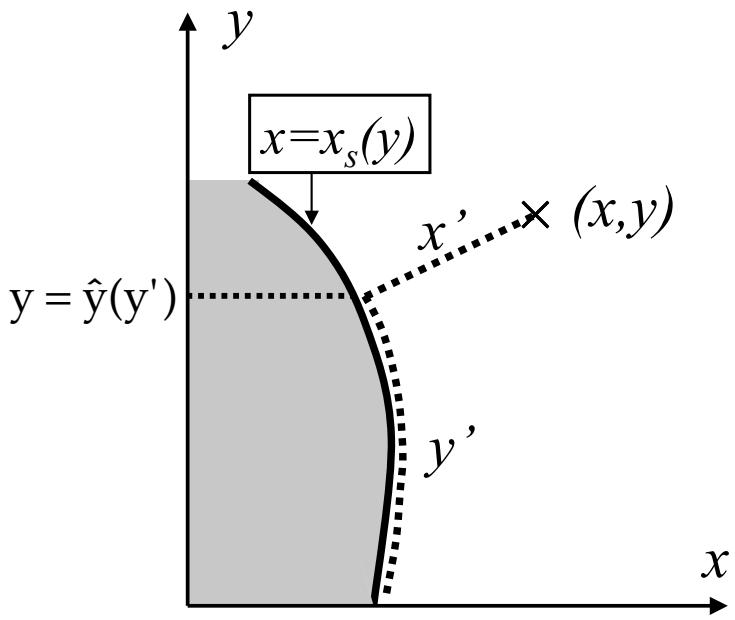

Figure 2: Curvilinear coordinate system associated to $x_s(y)$.

The angle between the local shoreline and the y axis is

$$\phi = tan^{-1}(\frac{dx_s}{dy}) \quad , \qquad -\frac{\pi}{2} < \phi < \frac{\pi}{2} \tag{4}$$

3.2 Curvilinear coordinate system

Given a particular shape of the the coastline, $x = x_s(y)$, a curvilinear coordinate system, x', y' will also be considered for some purposes. For each point (x, y) of the domain, let us consider the line from it up to the coastline which is perpendicular to the coastline. The distance from (x, y) to the intersection point is the x' coordinate. The distance along the coastline from this intersection point to the x axis is the y' coordinate. Provided that the radius of curvature of the shoreline at the embayments is large enough in comparison with the cross-shore length of the domain, L_x, no crossings will occur between the normal lines and the mapping will thereby be one-to-one.

The relationship between both coordinate systems is as follows. The alongshore

distance y' can be computed from its projection onto the y axis, $\hat{y}$, as

$$y' = \int_0^{\hat{y}} \sqrt{1 + (\frac{dx_s}{dy})^2} \quad dy \tag{5}$$

This defines the function $y' = \Psi(\hat{y})$ and the inverse function $\hat{y} = \Psi^{-1}(y') = F(y')$. Then from (x', y') we will have:

$$x = x_s(F(y')) + x' \cos\phi \quad , \quad y = F(y') - x' \sin\phi \tag{6}$$

Notice that

$$\cos\phi = \frac{1}{\sqrt{1 + (dx_s/dy)^2}} = \frac{dF}{dy'} \tag{7}$$

Therefore,

$$x = x_s(F(y')) + x' \frac{dF}{dy'} \quad , \quad y = F(y') - x' \sqrt{1 - (\frac{dF}{dy'})^2} \tag{8}$$

To invert eqs. 8 in order to provide (x', y') as a function of (x, y) the first step is realizing that those equations are nicely linear in x'. Therefore x' can be eliminated yielding a single equation in y' which reads:

$$y - F(y') + \{x - x_s(\, F(y')\,)\} \frac{\sqrt{1 - (\frac{dF}{dy'})^2}}{\frac{dF}{dy'}} = 0 \tag{9}$$

Now

$$\frac{\sqrt{1 - (\frac{dF}{dy'})^2}}{\frac{dF}{dy'}} = \tan\phi = \frac{dx_s}{d\hat{y}} \tag{10}$$

so that eq. 9 reads

$$y - F(y') + \{x - x_s(\, F(y')\,)\} \frac{dx_s}{d\hat{y}} = 0 \tag{11}$$

which can be finally cast into

$$y - \hat{y} + (x - x_s(\hat{y})) \frac{dx_s}{d\hat{y}}(\hat{y}) = 0 \tag{12}$$

This is an equation that can be solved numerically for $\hat{y}$ as a function of x and y giving rise to $\hat{y} = G(x, y)$ from where $y' = \Psi(\hat{y}) = \Psi(G(x, y))$. Once y' is known, x' can be readily computed from any of eqs. 8. Thus, the inverse mapping may be written as:

$$x' = (x - x_s(G(x, y)) \sqrt{1 + (dx_s/d\hat{y})^2} \quad , \quad y' = \Psi(G(x, y)) \tag{13}$$

Notice that the Newton solving of eq. 12 for each (x, y) can be done in the following way. For each y one can start at the shoreline, i.e., for $x = x_s(y) + \Delta x$ for which $\hat{y} \simeq y$. Then one can increase x cell by cell and initialize each Newton run with the previous one up to the maximum x which is needed.

For each (x, y), the angle ϕ is determined from eq. 7 once $\hat{y} = G(x, y)$ is known.

WARNING: For the first version of the model, the curvilinear coordinate system has not been used, i.e., it is assumed that $x' \simeq x$, $y' \simeq y$. In the second version, a different way to deal with large shoreline changes is set up in collaboration with A.B. Murray.

3.3 Equilibrium topography

The cross-shore equilibrium profile has a clear meaning for a rectilinear coastline. However, for a curvilinear coastline it is no so clear anymore. In principle one could assume that the bathymetry is defined by the equilibrium profile along the line which is perpendicular to the coastline at each coastline location. In other words, given a shape of the coastline, $x_s(y)$, each cross-shore section has an equilibrium beach profile, $z_e(x', x_s)$. Then, the 2DH equilibrium topography will be defined by $z = z_{be}(x', y') = z_e(x', x_s(\hat{y})) = z_e(x', x_s(F(y')))$. However, this option has a number of shortcomings. First, in case of a embayed coast, the cross-shore sections may intersect with the result that the bed level at the intersection may be double-valuated. Second, in this formulation the bed level at some offshore location does react to the position and shape of the shoreline. But this is actually non sense if the location is quite far offshore. The bed level will be a result of a balance between different sediment transport fluxes, mainly between *the local* onshore wave driven transport and down-slope gravitational transport. This has nothing to do with the coastline. Thus, the equilibrium profile should be found following wave rays in the seaward direction. This coincides, of course, with the shore-normal for rectilinear coastline under normal wave incidence. In general, since wave direction changes from one event to another, the most sensible assumption is to take the equilibrium profile along the mean cross-shore direction, that is, $z = z_{be}(x, y) = z_e(x, x_s(y))$.

The equilibrium profiles depend on the wave and sediment characteristics and various options can be used. As a starting point the simple shifted Dean profile used in *Falqués and Calvete* [2005] has been considered:

$$z_{be}(x, y) = -b\left((x + x_0 - x_s(y))^{2/3} - x_0^{2/3}\right) \tag{14}$$

The constants b and x_0 are determined in order to have a prescribed slope β at the coastline and a prescribed distance x_1 from the coastline to the location where the

water depth is, D_1. Thus, b and x_0 are solution of

$$\frac{2}{3}\, b\, x_0^{-1/3} = \beta \quad , \quad b\left((x_1 + x_0)^{2/3} - x_0^{2/3}\right) = D_1 \tag{15}$$

A longitudinal smoother has been applied in order to avoid offshore alongshore bathymetric gradients which are unrealistic. This smoother substitutes the bed level at each position (x, y) by the mean bed level between $(x, y - L_{sm})$ and $(x, y + L_{sm})$.

Regarding the dry beach it was initially assumed that the bed level was a fixed and uniform value, zb_{beach}. However, this produced some irregularities in the shoreline. Finally, a certain smooth profile for the subaereal beach has been assumed:

$$z_b(x, y) = zb_{beach}\left(1 - e^{\beta(x - x_s(y))/zb_{beach}}\right) \tag{16}$$

3.4 Wave driver

The wave driver computes the wave field, that is, wave height $H(x, y, t)$ and wave angle $\theta(x, y, t)$ from the wave height and angle at the offshore boundary (and upwaves lateral boundary).

3.4.1 Eikonal equation

A number of different wave drivers may be used but the simplest one that will be used by default is the one defined by the eikonal equations and the energy conservation:

$$\omega^2 = gk \tanh(kD) \tag{17}$$

$$\frac{\partial k_y}{\partial x} = \frac{\partial k_x}{\partial y} \tag{18}$$

$$\frac{\partial}{\partial x}(c_g H^2 \frac{k_x}{k}) + \frac{\partial}{\partial y}(c_g H^2 \frac{k_y}{k}) = 0 \tag{19}$$

Here, ω is the radian frequency, g is the gravity acceleration, $\vec{k} = (k_x, k_y) = k(-\cos\theta, \sin\theta)$ is the wavenumber vector and c_g is the group celerity. Eq. 17 is the dispersion relation, eq. 18 is the phase equation and eq. 19 is the energy conservation of the waves. Dissipation by bottom shear stress is neglected and there is no breaking dissipation since the wave field is needed only up to breaking.

The system of equations is decoupled. First, the modulus of the wavenumber, $k(x, y)$, can be computed from eq. 17. Then, from equation 18 one can determine the angle, $\theta(x, y)$. Finally, solving eq. 19 gives the wave height, $H(x, y)$.

Equation 17 is just algebraic and can be solved by a Newton-Raphson iterative scheme on the staggered grid (ic, jc), starting from the offshore boundary and progressing onshore. Thus, the changes from one point to the next one are very small and the method converges very quickly. At the offshore boundary the deep water approximation can be used to initialize.

Once $k(x, y)$ is known, k_x, k_y can be computed as follows. We define $\xi = k_y$ so that eq. 18 reads:

$$\frac{\partial \xi}{\partial x} = -\frac{\partial}{\partial y}\sqrt{k^2 - \xi^2} \tag{20}$$

The minus sign comes from $k_x = -\sqrt{k^2 - \xi^2}$. Equation 20 is discretized as:

$$\frac{\xi_{ic,jc} - \xi_{ic-1,jc}}{\Delta x} = -\frac{\sqrt{k^2_{ic,jc} - \xi^2_{ic,jc}} - \sqrt{k^2_{ic,jc-1} - \xi^2_{ic,jc-1}}}{\Delta y} \tag{21}$$

For the time being it is assumed that $\theta > 0$. The integration scheme must be done from the offshore boundary marching onshore. Thus, knowing line ic, line $ic - 1$ is computed by:

$$\xi_{ic-1,jc} = \xi_{ic,jc} + \frac{\Delta x}{\Delta y}\left(\sqrt{k^2_{ic,jc} - \xi^2_{ic,jc}} - \sqrt{k^2_{ic,jc-1} - \xi^2_{ic,jc-1}}\right) \tag{22}$$

Notice that apart from the values of ξ at the offshore boundary, $\xi_{n,jc}$, also their values at the $y = 0$ boundary, $\xi_{ic,1}$, must be known. Otherwise, at line $ic = n - 1$, $\xi_{n-1,1}$ would be unknown. At next line, $ic = n - 2$, $\xi_{n-2,1}$ and $\xi_{n-2,2}$ would remain unknown, and so on. Thus, there is a triangle next to the up-waves lateral boundary where ξ could not be determined.

In case of $\theta < 0$ the scheme is totally analogous but with a computational molecule based on $(ic, jc), (ic-1, jc), (ic, jc+1)$ instead of $(ic, jc), (ic-1, jc), (ic, jc-1)$. This reads:

$$\xi_{ic-1,jc} = \xi_{ic,jc} + \frac{\Delta x}{\Delta y}\left(\sqrt{k^2_{ic,jc+1} - \xi^2_{ic,jc+1}} - \sqrt{k^2_{ic,jc} - \xi^2_{ic,jc}}\right) \tag{23}$$

Finally, in case $\theta = 0$, eq. 22 can be used for $jc > 1$, except for $jc = 1$, for which eq. 23 is used. Once $\xi(x, y)$ is known, the angle can be computed from $\sin\theta = \xi/k$.

Well-posedness for hyperbolic equations requires that a ray entering the numerical cell trough its higher x basis do not go out through the lateral sides, parallel to y axis. Thus high incidence angles need a rectangular grid with $\Delta x < \Delta y$. Tests for parallel and rectilinear depth contours to check against Snell law show that $\Delta x = \Delta y$ works until $\theta_\infty \simeq 55^o$ and that it is possible to treat $\theta_\infty = 89^o$ with $\Delta y = 4\Delta x$.

Finally, to solve eq. 19 for $H(x, y)$, we can think of two options:

1. Equation 19 can be discretized as:

$$\frac{1}{2\Delta x}\left(c_g H^2 \frac{\sqrt{k^2-\xi^2}}{k}\Big|_{ic+1,jc} - c_g H^2 \frac{\sqrt{k^2-\xi^2}}{k}\Big|_{ic-1,jc}\right) - \frac{1}{2\Delta y}\left(c_g H^2 \frac{\xi}{k}\Big|_{ic,jc+1} - c_g H^2 \frac{\xi}{k}\Big|_{ic,jc-1}\right) = 0 \quad (24)$$

where the '$-$' sign comes from $k_x = -\sqrt{k^2-\xi^2}$. From this equation it readily follows:

$$H^2_{ic-1,jc} = \frac{k}{c_g\sqrt{k^2-\xi^2}}\Big|_{ic-1,jc} \left(c_g H^2 \frac{\sqrt{k^2-\xi^2}}{k}\Big|_{ic+1,jc} - \frac{\Delta x}{\Delta y}(c_g H^2 \frac{\xi}{k}\Big|_{ic,jc+1} - c_g H^2 \frac{\xi}{k}\Big|_{ic,jc-1})\right)$$

This scheme allows computing $H_{ic-1,jc}$ from H at rows ic and $ic+1$. Thus, $H(x,y)$ can be computed up to breaking by starting at the offshore boundary, $ic = n$, and marching onshore. There are however a number of details that should be fixed. First, the knowledge of H not only at $ic = n$ but also at $ic = n-1$ is needed. This can be solved by assuming that the alongshore gradients are negligible in deep water, $\partial(c_g H^2 \sin\theta)/\partial y \simeq 0$, so that $c_g H^2 \xi/k|_{n-1,jc} \simeq c_g H^2 \xi/k|_{n,jc}$. Second, to apply this scheme at the lateral boundaries, the information at $jc = 0$ and at $jc = m+1$ is required. In case $\theta \neq 0$, it will be assumed that $H(x,y)$ coincides with the undisturbed wave field at the up-waves lateral boundary and tends to the undisturbed wave field with relaxation distance λ_y at the down-waves boundary. Thus, if $\theta > 0$,

$$H_{ic,1} = H^e{}_{ic} \quad , \quad \frac{\partial}{\partial y}(c_g H^2 \frac{\xi}{k})\Big|_{ic,m} = -\lambda_y^{-1}\left(c_g H^2 \frac{\xi}{k})\Big|_{ic,m} - c_g H^2 \frac{\xi}{k}\Big|^{eq}_{ic}\right) \quad (25)$$

where $H^e_{ic}, c_{g^e_{ic}}, k^e_{ic}, \xi^e_{ic}$ are the wave quantities for the undisturbed equilibrium, $z_b = z_{be}(x)$. Similarly, for $\theta < 0$,

$$H_{ic,m} = H^e{}_{ic} \quad , \quad \frac{\partial}{\partial y}(c_g H^2 \frac{\xi}{k})\Big|_{ic,1} = \lambda_y^{-1}\left(c_g H^2 \frac{\xi}{k})\Big|_{ic,1} - c_g H^2 \frac{\xi}{k}\Big|^{eq}_{ic}\right) \quad (26)$$

In case $\theta = 0$, the tendency to the undisturbed wave field is assumed at both lateral boundaries, i.e., the second of each pair of those equalities will be considered.

2. The method just presented is not suited to arbitrarily shaped shorelines. In this case it is better to write eq. 19 as:

$$\nabla\cdot(H^2\vec{c}_g) = 0 \quad \Rightarrow \quad \vec{c}_g\cdot\nabla H^2 + H^2\nabla\cdot\vec{c}_g = 0 \quad \Rightarrow \quad c_g\frac{dH^2}{ds} + H^2\nabla\cdot\vec{c}_g = 0$$

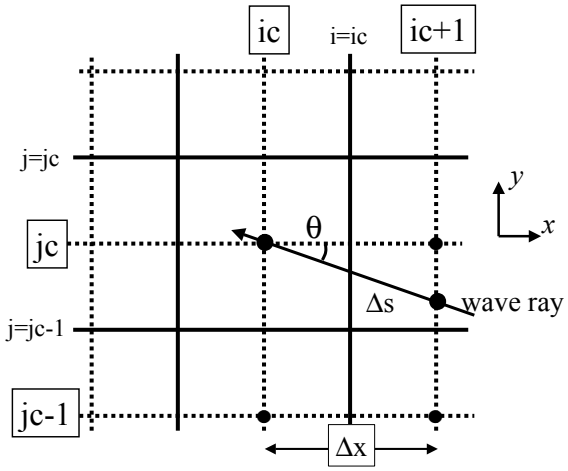

Figure 3: Computational molecule for the energy equation

where d/ds is the derivative along the wave rays. Now, by defining $\mathcal{E} = \ln(H^2)$ and $\Phi = -(\nabla \cdot \vec{c}_g)/c_g$ we finally obtain:

$$\frac{d\mathcal{E}}{ds} = \Phi \tag{27}$$

The discretization of eq. 27 will proceed by using the wave rays or characteristic lines. To compute $\mathcal{E}_{ic,jc}$ we will use the wave ray that crosses node (ic, jc) and that intersects the line $ic+1$ at the point $(x^*(ic+1), y^*(jc) - \Delta x \, \tan\theta)$ if $\tan(\theta) \leq \Delta y/\Delta x$. In case $\tan\theta > \Delta y/\Delta x$, the relevant intersection is with line $jc-1$ at the point $(x^*(ic) + \Delta y/\tan\theta, y^*(jc-1)$. Here, we define $x^*(ic) = (x(ic-1) + x(ic))/2$ and $y^*(jc) = (y(jc-1) + y(jc))/2$. Thus, if $|\tan(\theta)| \leq \Delta y/\Delta x$ eq. 27 can be approximated by:

$$\frac{\mathcal{E}_{ic,jc} - \mathcal{E}_{ic+1}(y_a)}{\Delta s} = \Phi_{i=ic}(y_b) \tag{28}$$

where

$$\mathcal{E}_{ic+1}(y_a) = \mathcal{E}_{ic+1,jc} + \frac{\mathcal{E}_{ic+1,jc-1} - \mathcal{E}_{ic+1,jc}}{\Delta y} \Delta x \, \tan\theta \tag{29}$$

is the linear interpolation of $\mathcal{E}$ along the line $x = x^*(ic+1)$. Similarly,

$$\Phi_{i=ic}(y_b) = \Phi_{ic,jc-1} + (\Delta y - \Delta x \, \tan\theta) \, \frac{\Phi_{ic,jc} - \Phi_{ic,jc-1}}{2\Delta y} \tag{30}$$

is the linear interpolation of Φ along the wave ray at its crossing with $x(i)$ for $i = ic$. In case $|\tan\theta| > \Delta y/\Delta x$, eq. 28 will be substituted by

$$\frac{\mathcal{E}_{ic,jc} - \mathcal{E}_{jc-1}(x_a)}{\Delta s} = \Phi_{j=jc-1}(x_b) \tag{31}$$

where

$$\mathcal{E}_{jc-1}(x_a) = \mathcal{E}_{ic,jc-1} + \frac{\mathcal{E}_{ic+1,jc-1} - \mathcal{E}_{ic,jc-1}}{\Delta x}\,\Delta y \,/\, \tan\theta \tag{32}$$

is the linear interpolation of $\mathcal{E}$ along the line $jc-1$. Likewise,

$$\Phi_{j=jc-1}(x_b) = \Phi_{ic,jc-1} + (\Delta x + \Delta y/\tan\theta)\,\frac{\Phi_{ic,jc-1} - \Phi_{ic-1,jc-1}}{2\Delta x} \tag{33}$$

From equations 28 or 31 $\mathcal{E}_{ic,jc}$ can be calculated from the knowledge of $\mathcal{E}$ on line $ic+1$. The previous knowledge of $\mathcal{E}_{ic,jc-1}$ is also required if $|\tan\theta| > \Delta y/\Delta x$. Thus, $\mathcal{E}$ can be computed by starting offshore with the smallest y and marching in the y-direction for each $x = const.$ line, and onshore from one $x = const.$ line to the next one.

The scheme just described can not be applied at the lateral boundaries ($y = const.$) at cells where the rays enter into the domain. For this case, it can be assumed that the missing information from outside the domain corresponds to an alongshore uniform equilibrium. Thus, an equilibrium line with bathymetry $z_b = z_{be}(x)$, wave height $H_e(x)$ defined by $H_e(x) = H_\infty \sqrt{(c_g\cos\theta)_\infty / c_g\cos\theta(x)}$ and the corresponding $\mathcal{E}(x), \Phi(x)$ is used to extract the necessary information from the lines next to the boundary, $jc = 0, jc = m+1$. Alternatively, a weaker version of such an assumption may be used. It consists of assuming that the wave field does not match with this equilibrium right at the boundaries but tends asymptotically to the equilibrium within a characteristic distance λ_y. For instance, for $H(x,y)$ at boundary $y = L_y$ this would mean

$$\frac{\partial H}{\partial y} = -\lambda_y^{-1}(H(x,y) - H_e(x)) \tag{34}$$

from where $H_{ic,m+1}$ can be computed as:

$$H_{ic,m+1} = H_{ic,m} - \lambda_y^{-1}(H_{ic,m} - (H_e)_{ic})\,\Delta y \tag{35}$$

We can proceed similarly with the other needed variables at both boundaries, $y = 0$ and $y = L_y$.

3.4.2 RefDif

Another option is using the RefDif program (ref.???, equation???). This is done by selecting the subroutine WAVES1 instead of WAVES. This subroutine calls 'mildsl.f' and 'refdif1m55.f'(Roland Garnier)where RefDif is included. The files param.fi, parcon.fi and refdif1m55.fi are used (morfo55 model).

3.5 Wave breaking

Once the wave field $H(x,y), \theta(x,y)$ is known, the wave height H_b and wave angle θ_b at breaking are determined on the rectangular grid $(x-y)$ (central points ic, jc) as follows. For each y, the highest x such that $H(x,y) \geq \gamma_b D(x,y)$ is seek for. This defines $x_b = x_b(y)$ and thereby $H_b(y) = H(x_b, y)$, $\theta_b(y) = \theta(x_b, y)$. Then by using the inverse mapping eqs. 13, $x'_b = x'(x_b, y), y' = y'(x_b, y)$ the pairs x'_b, y' define

$$X_b(y') = x'_b(y') \tag{36}$$

This also defines $H_b = H_b(y')$, $\theta_b = \theta_b(y')$.

3.6 Dynamical equation: sediment conservation

The dynamical equation in the model is the sediment conservation

$$\frac{\partial z_b}{\partial t} + \frac{\partial q_x}{\partial x} + \frac{\partial q_y}{\partial y} = 0 \tag{37}$$

where $\vec{q}$ is the horizontal depth-integrated sediment flux $(m^3/m/s)$. The porosity factor is included in the expression of $\vec{q}$ as $1/(1-p)$. This equation is discretized on all the wet cells, $ic \geq ishore(jc)$, by using an explicit second order Adam-Bashforth scheme in time [*Caballeria et al.*, 2002] and finite differences in space:

$$zb^k_{ic,jc} = zb^{k-1}_{ic,jc} - (\frac{3}{2}\, div^{k-1}_{ic,jc} - \frac{1}{2}\, div^{k-2}_{ic,jc})\, \Delta t \tag{38}$$

with

$$1 \leq jc \leq m\,, \quad ishore(jc) \leq ic \leq n\,, \quad k \geq 2 \tag{39}$$

and

$$div^k_{ic,jc} = \frac{q_x(i,jc)^k - q_x(i-1,jc)^k}{\Delta x} + \frac{q_y(ic,j)^k - q_y(ic,j-1)^k}{\Delta y} \tag{40}$$

with

$$1 \leq jc \leq m\,, \quad ishore(j) \leq ic \leq n\,, \quad i = ic\,, \quad j = jc\,, \quad k \geq 0 \tag{41}$$

3.7 Sediment transport

The sediment flux

$$\vec{q} = \vec{q}_{CERC} + \vec{q}_{DIFF} \tag{42}$$

consists of two terms, the alongshore wave-driven flux $\vec{q}_{CERC}$ and the flux corresponding to the transport commonly known as 'cross-shore', $\vec{q}_{DIFF}$.

3.7.1 Wave-driven alongshore transport

The wave-driven alongshore transport is computed as a cross-shore distribution of the total transport rate

$$q_{y'}(x,y) = f(x')Q(y') \tag{43}$$

where (x,y) are the cartesian coordinates, (x',y') are the curvilinear coordinates, $f(x')$ is the normalized cross-shore distribution function with

$$\int_0^\infty f(x')\,dx' = 1 \tag{44}$$

and Q is the total transport rate (m^3/s). Notice that the computation of longshore transport first requires using the inverse mapping eq. 13 to determine (x',y') from (x,y).

The generalized CERC formula for the transport rate [*Komar*, 1998; *Horikawa*, 1988]

$$Q = \mu H_b^{5/2}\left(\sin(2\alpha_b) - \frac{2r}{\beta}\cos(\alpha_b)\frac{\partial H_b}{\partial y'}\right) \tag{45}$$

is here considered where $H_b(y')$ is the (rms) wave height and $\alpha_b = \theta_b(y') - \phi(y')$ is the angle between wave fronts and coastline at breaking. The constant in front of it is of order $\mu \sim 0.1 - 0.2$ $\mathrm{m}^{1/2}\mathrm{s}^{-1}$ and β is the beach slope at the shoreline. The value $r = 1$ has been used.

To compute the sediment flux, the angle $\phi(y')$ is actually substituted by the angle between the y-axis and the 'mean shore orientation'. This orientation is defined as an average between that of the shoreline (with weight m_1) and the mean orientation of ∇z_b in the surf zone (with weight m_2), with $m_1 + m_2 = 1$. In other words,

$$\bar{\phi}(y') = \tan^{-1}(m_1\tan(\phi(y')) + m_2\tan(\phi_{surf}(y')) \tag{46}$$

where

$$\sin\phi_{surf}(y') = \frac{\frac{\partial \bar{z}_b}{\partial y}}{\sqrt{(\frac{\partial \bar{z}_b}{\partial y})^2 + (\frac{\partial \bar{z}_b}{\partial x})^2}} \tag{47}$$

This direction tries to parameterize the direction of the shoreline actually felt by the waves. The angle $\phi(y')$ of the shoreline is computed not directly with dx_s^*/dy' but with the linear regression of the points $(y'_j, x_s^*(y'_j))$ with $y' - L_{sm} \le y'_j \le y' + L_{sm}$.

Based on the profile of the longshore current there are several options for the distribution function (*Komar* [1998], chap.9). As a first instance we will use a function which is qualitatively realistic:

$$f(x') = \frac{4}{\sqrt{\pi}L^3}x'^2\,e^{-(x'/L)^2} \tag{48}$$

with $L = 0.7X_b(y')$, where $X_b(y')$ is the width of the surf zone at the alongshore position y'.

Given that the sediment transport at the swash zone may be significant [*Komar*, 1998], this expression has been later extended to:

$$f(x') = A\left(b + \frac{4}{\sqrt{\pi}L^3}x'^2\right) e^{-(x'/L)^2} \tag{49}$$

with $f'(0) = Ab \neq 0$. The normalization condition, eq. 44, implies:

$$A = \frac{2}{2 + bL\sqrt{\pi}} \tag{50}$$

Then, the value of $f'(0)$ at the shoreline is forced to be a fraction ρ of the maximum of $f'(x)$, which implies:

$$\frac{\sqrt{\pi}}{4} bL\, e^{1-bL\sqrt{\pi}/4} = \rho \tag{51}$$

Then, $\rho = 0.5 \Rightarrow bL = 0.5191$, $\rho = 0.4 \Rightarrow bL = 0.3836$, $\rho = 0.3 \Rightarrow bL = 0.2708$ and $\rho = 0.1 \Rightarrow bL = 0.0903$.

Finally, the alongshore sediment flux $q_{y'}$ is projected onto the x and y axis to give:

$$\vec{q}_{CERC} = f(x')Q(y')\,(\cos\phi(y'), \sin\phi(y') \tag{52}$$

where the angle $\phi(y')$ is given by eq. 7.

3.7.2 'Cross-shore' transport. Tendency to an equilibrium profile.

The second term in eq. 42 is an attempt to parameterize the cross-shore processes that bring the cross-shore profiles to equilibrium. This parameterization poses a difficult election. Two options have been considered:

1. In a first instance,
$$\vec{q}_{DIFF} = -\gamma\nabla(z_b - z_{be}) \tag{53}$$
has been assumed, where $z_{be}(x, y)$ is the equilibrium bathymetry which depends on wave and sediment characteristics. This sediment transport diffuses away the departures from the equilibrium topography with a diffusivity γ which may be a function of different variables like the distance to shore $x - x_s$ and wave height H. The γ factor may be an anisotropic second order tensor, the diffusivity being different in the alongshore or the cross-shore directions.

2. In the first option the equilibrium bathymetry at some offshore location depends on the position and orientation of the coastline rather than depending only on the local processes at this location. Since this makes little sense (see discussion in Sec. 3.3), another option has been considered in which the sediment flux reads:

$$\{\vec{q}_{DIFF}\}_x = -\gamma_x(\frac{\partial z_b}{\partial x} - s_e) \quad , \quad \{\vec{q}_{DIFF}\}_y = -\gamma_y \frac{\partial z_b}{\partial y} \tag{54}$$

where the equilibrium cross-shore slope s_e can be computed as a function of water depth D, wave height H, etc. by using any representation of equilibrium profiles. For instance by using the profile, $D = b((x+x_0)^{2/3} - x_0^{2/3})$ introduced in Sec. 3.3, it follows

$$s_e = -\frac{2}{3}\frac{b^{3/2}}{\sqrt{D + bx_0^{2/3}}} \tag{55}$$

To parameterize γ_x, γ_y there are several options. One option would be using the downslope transport term of the Bailard formulation. Here we have chosen a diffusivity which is proportional to the turbulent diffusivity in the momentum equations, $\nu_t = M(\mathcal{D}/\rho)^{1/3} H_{rms}$. The average wave dissipation in the surf zone can be estimated as

$$\mathcal{D} \sim \frac{1}{8}\rho g H_b^2 \frac{c_{gb}}{X_b} \sim \frac{1}{8}\rho g H_b^2 \frac{\sqrt{gD_b}}{X_b} \tag{56}$$

Then, we define the diffusivities ϵ_x, ϵ_y as proportional to the average ν_t with global nondimensional factors, $\epsilon_{xm}, \epsilon_{ym}$, and a shape function that makes the diffusivity significant near the shore up to a distance x_1 and makes it to decay offshore up to a residual value:

$$\epsilon_x(x) = \epsilon_{xm}\, g^{1/2} H_b^{11/6} \gamma_b^{-1/6} X_b^{-1/3} \frac{1 + b + \tanh((x_1 - x)/L_d)}{1 + b + \tanh(x_1/L_d)} \tag{57}$$

$$\epsilon_y(x) = \epsilon_{ym}\, g^{1/2} H_b^{11/6} \gamma_b^{-1/6} X_b^{-1/3} \frac{1 + b + \tanh((x_1 - x)/L_d)}{1 + b + \tanh(x_1/L_d)} \tag{58}$$

The decay distance is $\sim L_d = 0.4x_1$. The constant b is related to the residual value, so that:

$$b = \frac{1 + \tanh(x_1/L_d)}{1 - \epsilon_{xmin}/\epsilon_{xm}} \frac{\epsilon_{xmin}}{\epsilon_{xm}} \tag{59}$$

with $\epsilon_{xmin}/\epsilon_{xm} = \epsilon_{ymin}/\epsilon_{ym} = 0.1$.

Actually, ϵ_x is multiplied by a factor

$$\sqrt{(x - x_s)/X_b}$$

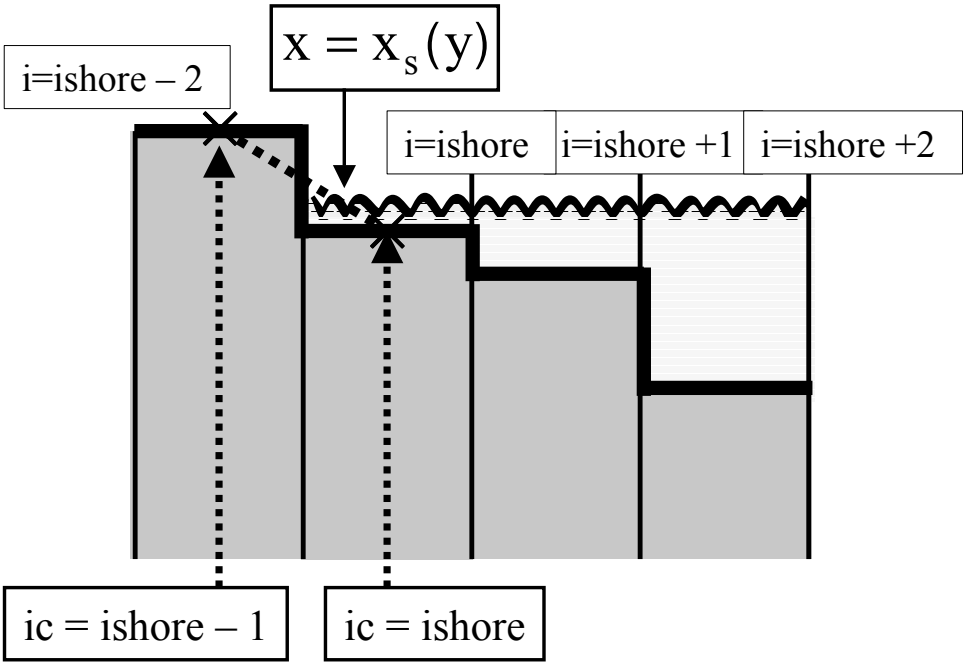

Figure 4: Cross-shore section of the discretized topography, dry cells, wet cells and shoreline.

3.7.3 'Cross-shore' transport. Parameterization of the 'wave-driven onshore transport'.

This option consists in adding up two terms: one in the direction of wave propagation which accounts for the transport caused by wave nonlinearities (parameterized, e.g., by Bailard) and a second one which is purely downslope:

$$\vec{q} = -\gamma \nabla z_b \tag{60}$$

This option will be implemented soon ???.

3.8 Coastline evolution

Before explaining the general 2D case it is first convenient to show the rationale in the simpler case of a rectilinear coastline.

3.8.1 Simplest case: rectilinear coastline

At each time step, the coastline updating is achieved in four steps:

1. The sediment conservation law eq. 38 is applied to find the updated bathymetry $zb^k_{ic,jc}$ from the bathymetries at time steps $k-1$ and $k-2$. This is done in all the wet cells including the cells next to the shoreline, i.e., the cells between $i = ishore - 1$ and $i = ishore$ (we omit the j index since we as yet ignore any dependency in y).

2. The new position of the shoreline, $ic = ishore$ and $x = x_s(y)$ is determined as explained in Sec. 3.1. In the previous step, no dry cells can change, but it may happen that wet cells become dry if there is accretion, $\Delta z_b > 0$. Thus, in this step, the shoreline either keeps its position or advances seaward.

3. Now the bed slope at the shoreline is corrected to avoid an unrealistically steep slope. To this end, two slopes are given from the input data: the maximum allowed slope, β_{cri}, and the prescribed slope, $\beta_1 \leq \beta_{cri}$. First, the slope resulting from the previous steps is computed:

$$\beta = \frac{zb_{ishore-1} - zb_{ishore}}{\Delta x} \tag{61}$$

   Then, if $\beta \leq \beta_{cri}$ the topography and shoreline position are kept as they stand. Otherwise, if $\beta > \beta_{cri}$ the topography at both sides of the shoreline is corrected so as to get a bed slope β_1 at the swash zone. This is done as follows. The previous topography is represented by zb and the corrected one by zb'. For simplicity, $ishore = ic$. Then the equations are:

$$\frac{zb'_{ic-1} - zb'_{ic}}{\Delta x} = \beta_1 \qquad , \qquad zb'_{ic} - zb_{ic} = -(zb'_{ic-1} - zb_{ic-1}) \tag{62}$$

   The second equation sets the conservation of sediment: some sediment is removed from the landward cell and is entirely deposited in the seaward cell. This system is readily solved for the updated topography:

$$zb'_{ic} = \bar{zb} - \frac{1}{2}\beta_1 \Delta x \qquad , \qquad zb'_{ic-1} = \bar{zb} + \frac{1}{2}\beta_1 \Delta x \tag{63}$$

   where $\bar{zb} = (zb_{ic} + zb_{ic-1})/2$.

4. Step 2 is repeated to find the new position of the shoreline caused by the rearrangement of the topography performed in step 3. The shoreline may stay or may move but now, if it moves, it may either advance or retreat.

The prescribed slope may be computed with the empirical expression of Sunamura (see *Short* [1999], pag. 128)

$$\beta_1 = 0.12 g D_s \left(\frac{T}{H_b}\right)^2 \tag{64}$$

where D_s is the sediment grain diameter.

3.8.2 General case

Let us now apply the ideas developed for the rectilinear coast to the general case. The steps 1, 2 and 4 in which eq. 38 is applied and the shoreline position is determined will be the same. Step 3 will change to adapt to 2D the correction of the bed slope at the swash zone.

Given a jc let us assume first that $\tan\phi = dx_s/dy > 0$ for $y(jc)$. In case $dx_s/dy = 0$ the shoreline is updated as explained in Sec. 3.8.1. The case $dx_s/dy < 0$ is similar to that one and will be discussed later on.

For simplicity, $ishore(jc) = ic$. The initial bed slope is computed as

$$\beta = (-\cos\phi, \sin\phi) \cdot \nabla z_b \tag{65}$$

where the gradient is approximated by

$$\nabla z_b \simeq \left(\frac{zb_{ic,jc} - zb_{ic-1,jc}}{\Delta x}\,,\ \frac{zb_{ic,jc+1} - zb_{ic,jc}}{\Delta y} \right) \tag{66}$$

Now, if $\beta \leq \beta_{cri}$ the topography and shoreline position are kept as they stand at this alongshore position. If $\beta > \beta_{cri}$ the topography will be changed to get the prescribed slope β_1.

The idea is that the bottom surface must be locally rotated around the local shoreline in order to reduce the slope in the cross-shore direction. Numerically, this involves the central grid points $(ic, jc), (ic-1, jc)$ and $(ic, jc+1)$ so that the bed level at these points will be modified in order to get the β_1 slope at the swash zone. Let zb be the initial bed levels, zb' the updated ones and $\bar{zb} = (zb_{ic,jc} + zb_{ic-1,jc} + zb_{ic,jc+1})/3$. Then the sediment conservation reads:

$$zb'_{ic,jc} + zb'_{ic-1,jc} + zb'_{ic,jc+1} = 3\bar{zb} \tag{67}$$

The condition that the new cross-shore slope is β_1 reads:

$$-\frac{zb'_{ic,jc} - zb'_{ic-1,jc}}{\Delta x}\cos\phi + \frac{zb'_{ic,jc+1} - zb'_{ic,jc}}{\Delta y}\sin\phi = \beta_1 \tag{68}$$

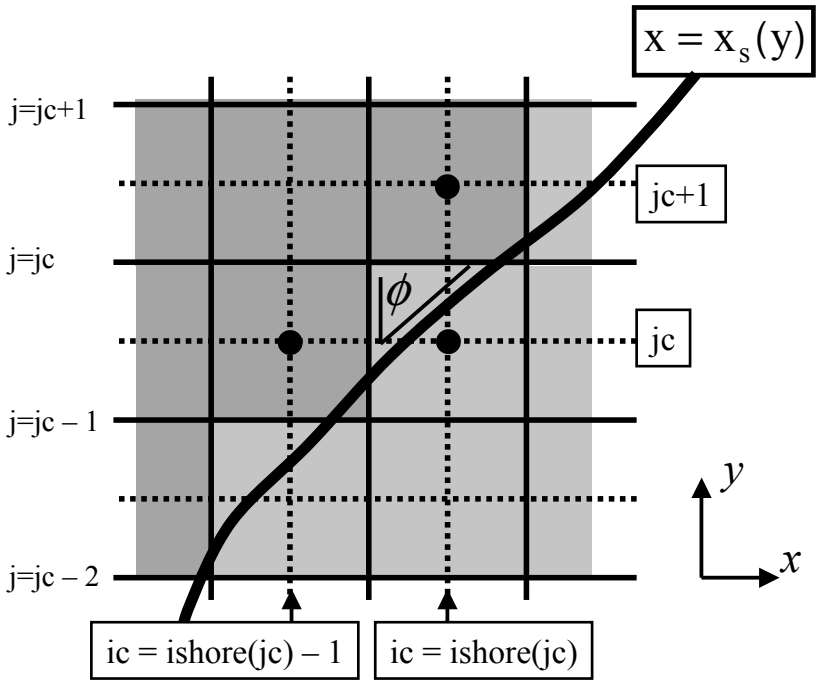

Figure 5: Correction on the bed slope at the shoreline.

Finally, the alongshore slope must be zero since the rotation axis is the shoreline:

$$\frac{zb'_{ic,jc} - zb'_{ic-1,jc}}{\Delta x}\sin\phi + \frac{zb'_{ic,jc+1} - zb'_{ic,jc}}{\Delta y}\cos\phi = 0 \tag{69}$$

This poses a system of three linear equations for the updated bed levels which is readily solved to give:

$$\begin{aligned} zb'_{ic,jc} &= \bar{zb} - \frac{\Delta x}{3}\beta_1\cos\phi - \frac{\Delta y}{3}\beta_1\sin\phi \\ zb'_{ic-1,jc} &= \bar{zb} + \frac{2\Delta x}{3}\beta_1\cos\phi - \frac{\Delta y}{3}\beta_1\sin\phi \\ zb'_{ic,jc+1} &= \bar{zb} - \frac{\Delta x}{3}\beta_1\cos\phi + \frac{2\Delta y}{3}\beta_1\sin\phi \end{aligned} \tag{70}$$

In case where $\tan\phi = dx_s/dy < 0$ for $y(jc)$, the procedure is totally similar but the grid points involved are $(ic, jc), (ic-1, jc)$ and $(ic, jc-1)$. The system to solve is

$$zb'_{ic,jc} + zb'_{ic-1,jc} + zb'_{ic,jc-1} = 3\bar{zb} \tag{71}$$

$$-\frac{zb'_{ic,jc} - zb'_{ic-1,jc}}{\Delta x}\cos\phi + \frac{zb'_{ic,jc} - zb'_{ic,jc-1}}{\Delta y}\sin\phi = \beta_1 \tag{72}$$

$$\frac{zb'_{ic,jc} - zb'_{ic-1,jc}}{\Delta x}\sin\phi + \frac{zb'_{ic,jc} - zb'_{ic,jc-1}}{\Delta y}\cos\phi = 0 \tag{73}$$

and the solution is:

$$\begin{aligned} zb'_{ic,jc} &= \bar{zb} - \frac{\Delta x}{3}\beta_1\cos\phi + \frac{\Delta y}{3}\beta_1\sin\phi \\ zb'_{ic-1,jc} &= \bar{zb} + \frac{2\Delta x}{3}\beta_1\cos\phi + \frac{\Delta y}{3}\beta_1\sin\phi \\ zb'_{ic,jc+1} &= \bar{zb} - \frac{\Delta x}{3}\beta_1\cos\phi - \frac{2\Delta y}{3}\beta_1\sin\phi \end{aligned} \tag{74}$$

A longitudinal smoother has been applied to $x_s(y)$ which substitutes the shoreline displacement at each alongshore position (y) by its mean between $y - L_{sm}$ and $y + L_{sm}$.

There is the option of making $dz_b/dx = \beta_1$ always regardless β_{cri}. ???

3.9 The evolution problem

Since the 'cross-shore' transport depends on ∇z_b the governing equation 37 is second order in z_b of the parabolic type. For instance, in case of choosing the second option

for the 'cross-shore' transport, the dynamic equation reads:

$$\frac{\partial z_b}{\partial t} - \frac{\partial}{\partial x}\left(\gamma_x \frac{\partial z_b}{\partial x}\right) - \frac{\partial}{\partial y}\left(\gamma_y \frac{\partial z_b}{\partial y}\right) = -\frac{\partial}{\partial x}(\gamma_x s_e) - \nabla \cdot \vec{q}_{CERC} \tag{75}$$

Notice however that this equation is non-local. Indeed, although $\vec{q}_{CERC}$ at a given (x, y) depends on the local wave conditions, these depend on the bathymetry in all the domain via wave propagation from deep water (wave driver). Furthermore, γ_x, γ_y and s_e depend in general on wave height which in turn depends again on $z_b(x, y)$ in all the domain. Besides, equation 75 is highly nonlinear. Non-linearities arise because γ_x, γ_y and s_e depend on z_b. Furthermore, the CERC formula depends non-linearly upon ϕ, H_b and θ_b.

3.10 Boundary conditions

According to the parabolic type dictated by the dependence in t and the higher order derivatives of $z_b(x, y, t)$ in the equation, appropriate b.c. seem to be Dirichlet, Newman or mixed in the entire boundary. Our modelling approach is aimed at studying phenomena which are localized within a stretch of coast by using a finite domain. The domain has to be substantially larger than the area of interest and it is assumed that at the lateral boundaries the state of the system tends to an undisturbed equilibrium situation. Thus, appropriate Dirichlet b.c. would be:

$$z_b(x, 0) = z_{be}(x, 0) \qquad , \qquad z_b(x, L_y) = z_{be}(x, L_y) \tag{76}$$

The Dirichlet conditions are controlled through the TIMESTEP subroutines.

Newman or mixed conditions are based on the sediment flux and are therefore imposed in the SEDTRANS subroutines. Thus, several options can be considered according to the choice for the 'cross-shore' transport:

1. For the first option, eq. 60,

$$\vec{q}_{DIFF} = -\gamma \nabla (z_b - z_{be}) \tag{77}$$

   it is assumed that the bathymetry relaxes to the equilibrium bathymetry within a certain decay distance λ off the boundary. For instance, for the offshore boundary, $x = L_x$, this b.c. reads

$$\frac{\partial (z_b - z_{be})}{\partial x} = -\lambda_x^{-1}(z_b - z_{be}) \tag{78}$$

   which can also be written as

$$\{q_{DIFF}\}_x = \gamma_x \lambda_x^{-1}(z_b - z_{be}) \tag{79}$$

Similar conditions are assumed at the lateral boundaries which can be written as

$$\{q_{DIFF}\}_y = -\gamma_y \lambda_y^{-1}(z_b - z_{be}) \; : \qquad y = 0 \tag{80}$$

$$\{q_{DIFF}\}_y = \gamma_y \lambda_y^{-1}(z_b - z_{be}) \; : \qquad y = L_y \tag{81}$$

At the shore boundary, the condition $\{q_{DIFF}\}_x = 0$ is implicit in the rule for shoreline evolution eq. 67 or eq. 71. If there is a prescribed and non-vanishing sediment flux at the shoreline, this can be imposed in these equations by modifying $\bar{zb}$ so as to include the effect of the sediment flux in it.

2. For the second option, eq. 54,

$$\{\vec{q}_{DIFF}\}_x = -\gamma_x(\frac{\partial z_b}{\partial x} - s_e) \quad , \quad \{\vec{q}_{DIFF}\}_y = -\gamma_y \frac{\partial z_b}{\partial y} \tag{82}$$

the b.c. should be

$$\frac{\partial}{\partial x}\left(\frac{\partial z_b}{\partial x} - s_e\right) = -\lambda_x^{-1}(\frac{\partial z_b}{\partial x} - s_e) \tag{83}$$

but this would lead to a second order b.c. which is incompatible with a second order differential equation. Thus, at the offshore boundary we will impose the same b.c. as in the first case, eq. 79. At the lateral boundaries we will apply

$$\{q_{DIFF}\}_y = -\gamma_y \lambda_y^{-1}(z_b - z_{be}) \; : \qquad y = 0 \tag{84}$$

$$\{q_{DIFF}\}_y = \gamma_y \lambda_y^{-1}(z_b - z_{be}) \; : \qquad y = L_y \tag{85}$$

3.11 Coastal structures

The beach geometry in the model can include a number of emerged groins which are parallel to the x axis. Each groin has a width of Δy, between $j = jgroin(k)$ and $j = jgroin(k) + 1$ (for groin number k). The cross-shore tip of the groin is at $x = L_g(k)$ and in the discretization it is assumed that the groin ends at $i = igroin(k)$ which is the maximum i such that $x(i) \leq L_g(k)$. The effect of a groin in the morphodynamic problem is first an obstruction for sediment transport, namely:

$$\begin{aligned} q_y &= 0 \; : \qquad j = jgroin(k), \quad j = jgroin(k) + 1 \\ q_x &= 0 \; : \qquad i = igroin(k) \end{aligned} \tag{86}$$

The discretized sediment conservation equation is not considered over the groin, i.e., at $jc = jgroin(k) + 1$ for any $ic \leq igroin(k)$. The topographic level inside the groin is set to a constant positive value, $z_g > 0$. The possible hydrodynamic effects like shadowing or diffraction of the waves are discussed in Sec. 3.4.

This setup has been removed and a new way of dealing with groins is now being implemented to be applied to La Barceloneta beach (Barcelona).

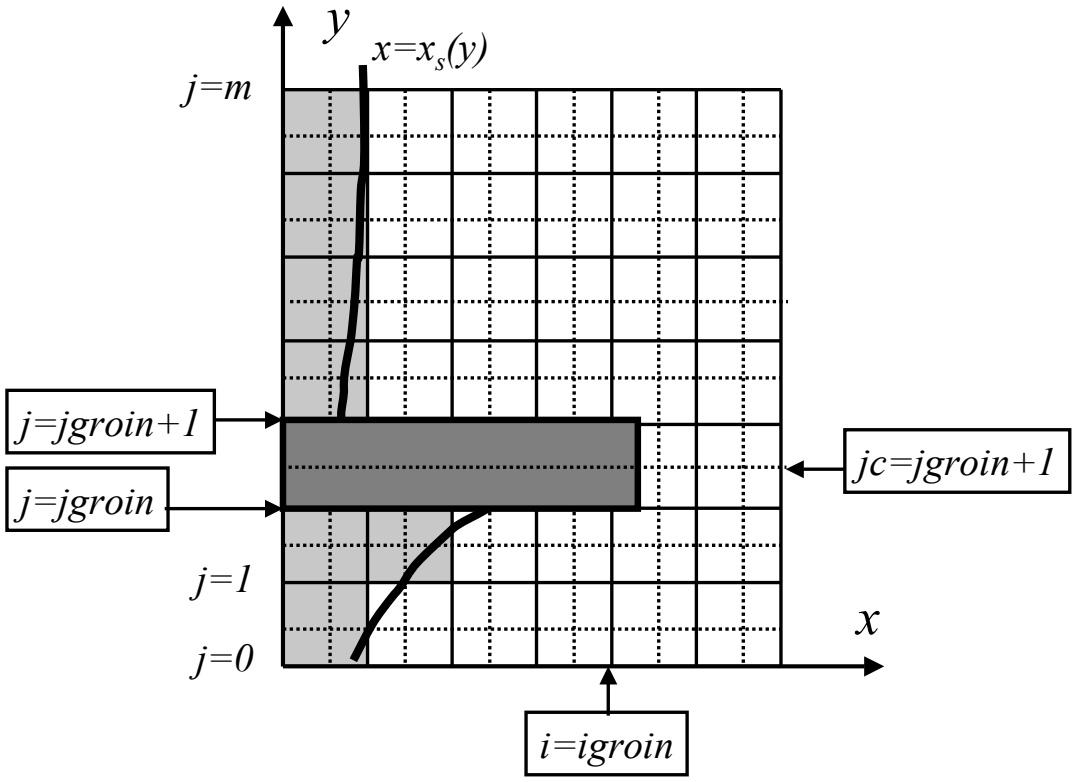

Figure 6: Discretization of a groin

4 The fortran code

The code is written in Fortran77. The input data are first read from the 'parama.dat' file and several constants are defined.

Then, there is a first run from $t = 0$ to $t = \Delta t$ which is different from the subsequent runs. First, the grid and the offshore wave conditions are defined (subroutines GRIDDING and OFFSHOREWAVE). Afterwards, the initial bathymetry is defined, either by using INIBATHY (if $nc(1) = 0$) or reading it from 'joint.dat' if we want to continue the previous run ($nc(1) \neq 0$). The initial bathymetry is output in 'topo0.dat'. Now, the wave field is computed (WAVES) and the breaking line and waves at breaking are determined (BREAKING). Also, the shoreline is defined (SHORELINE), the equilibrium bathymetry is obtained (EQUILIBRIUM) and the sediment flux along with its divergence is evaluated (SEDTRANS). Cross-shore or longshore profiles of some variables are now written. Finally the time step from $zb(x, y, 0)$ to $zb(x, y, \Delta t)$ is carried out in TIMESTEP0.

The normal runs for $t > \Delta t$ proceed as follows. OFFSHOREWAVE, WAVES, BREAKING, EQUILIBRIUM and SEDTRANS are called to define the offshore wave conditions and compute the wave field, breaking waves, equilibrium bathymetry, sediment flux and its divergence. Then, TIMESTEP computes $zb(x, y, t)$ from $z_b(x, y, t-\Delta t)$ and $z_b(x, y, t-2\Delta t)$. Afterwards, the cross-shore or longshore profiles of some variables are written and, finally, the 2D topography $z_b(x, y, t)$ is written in a 'topo*.dat' file. After doing all these actions the code goes back to call OFFSHOREWAVE, WAVES, BREAKING, etc. in a loop. The outputs are written only for some time steps which have been previously selected.

After arriving at the final computation time, the 'joint.dat' file is created in order to go on with the simulation if desired.

5 Basic case study and calibration: Evolution of a cuspate foreland/embayment and coastline diffusivity

A first test on Q2D-morfo is comparing the time scale of the smoothing of a cuspate foreland against the prediction provided by the traditional one-line modelling. Wave transformation effects are not accounted for in these experiments as in case of the traditional one-line modelling. This means that the wave height and direction at breaking are given as data, they do not change as a function of the morphological evolution.

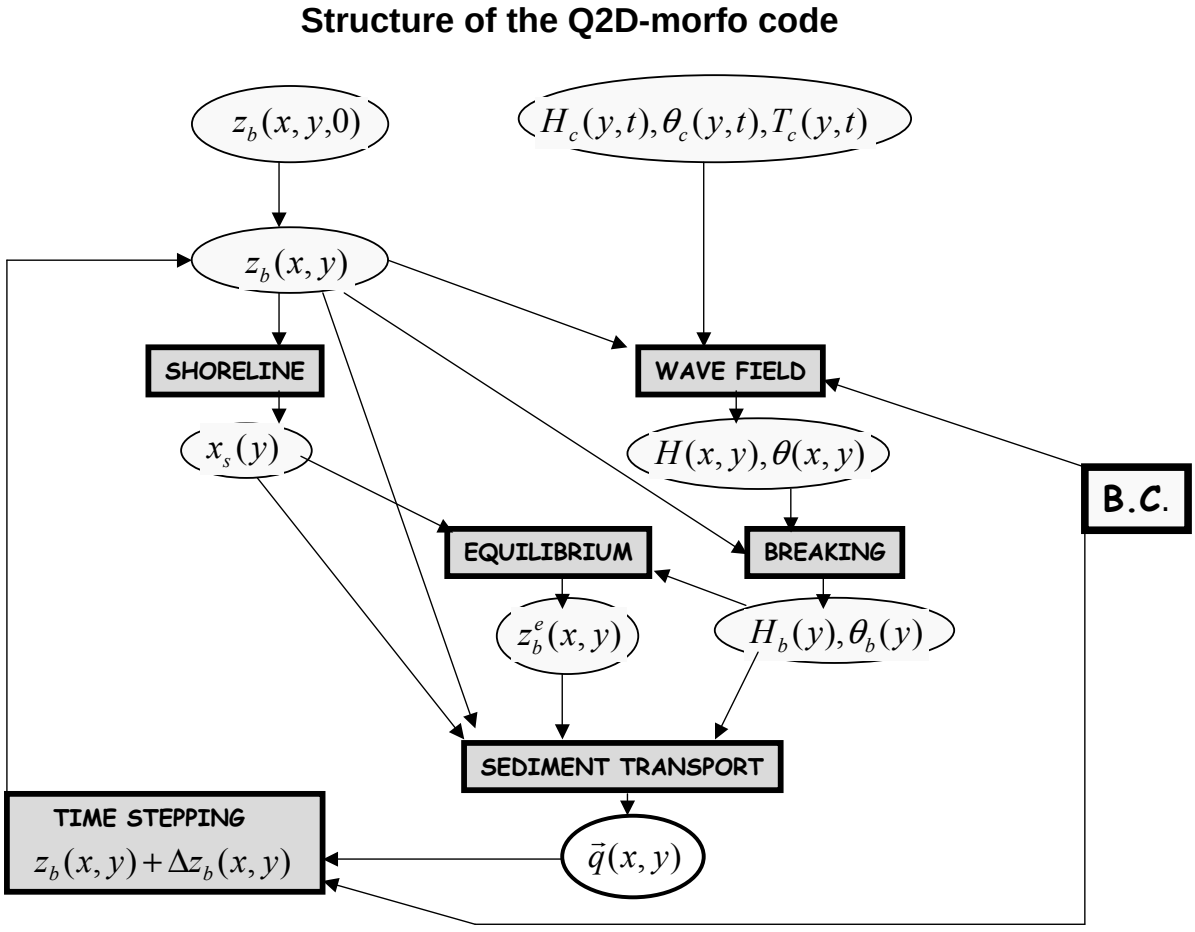

Figure 7: Structure of the fortran code.

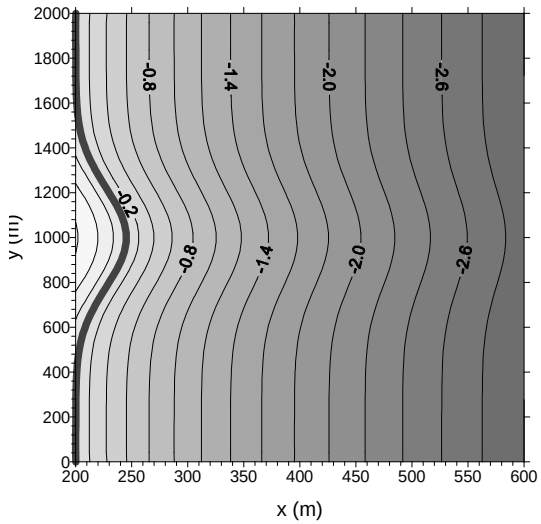

Figure 8: Initial shoreline and nearshore bathymetry for $D_c = 5$ m. Notice that the cross-shore distance has been magnified.

We will consider a perturbed coastline

$$x_s(y,0) = Ae^{-((y-y_a)/L)^2} \tag{87}$$

with an associated bathymetry

$$z_{b0}(x,y,0) = p(x)\, z'_{be}(x,y) + (1-p(x)) z_{be}(x) \tag{88}$$

which is an average between the equilibrium bathymetry associated to the unperturbed rectilinear coastline $x_s = \bar{x}_s = const.$

$$z_{be}(x) = -b\left((x + x_0 - \bar{x}_s)^{2/3} - x_0^{2/3}\right) \tag{89}$$

and the equilibrium bathymetry associated to the perturbed coastline

$$z'_{be}(x,y) = -b\left((x + x_0 - x_s(y,0))^{2/3} - x_0^{2/3}\right) \tag{90}$$

with a weight

$$p(x) = \frac{D_c + z_{be}(x)}{D_c} \quad if - z_{be}(x) < D_c \qquad and \qquad p = 0 \quad otherwise. \tag{91}$$

The depth D_c is a the depth of closure of the perturbation.

Table 1: Default parameters

Beach characteristics	L_x (m)	L_y (m)	$\bar{x}_s$ (m)	β_1	β_{cri}	β_0	L_1 (m)	D_1 (m)
	2000	2000	200	0.02	0.02	0.02	3000	12

Sediment Transport	μ $(m^{1/2}s^{-1})$	r	ϵ_{xm}	ϵ_{ym}	X_1	L
	0.15	1	0.1	0.03	$4X_b$	$0.7X_b$

Discretization	n	m	Δx (m)	Δy (m)	Δt (days)	λ_x (m)	λ_y (m)	m_2
	200	200	10	10	0.001	2000	2000	1

Perturbation and waves	y_a (m)	L (m)	D_c (m)	H_b (m)	θ_b
	1000	300	5	1	0

The equation governing the coastline position for the one line model is a diffusion one:

$$\frac{\partial x_s}{\partial t} = \epsilon \frac{\partial^2 x_s}{\partial y^2} \tag{92}$$

where the diffusivity is:

$$\epsilon = \epsilon_{cla} = 2\mu \frac{H_b^{5/2}}{\bar{D}} \cos(2\theta_b) \tag{93}$$

with $\bar{D}$ being an equivalent mean water depth for shoreline change. This depth gives the sand volume $\Delta V = \bar{D}\Delta y \Delta x_s$ involved in a change Δx_s of shoreline position along a stretch Δy of coast. Equation 92 with B.C. $x_s(-\infty, t) = x_s(+\infty, t) = 0$ and initial condition eq. 87 can be solved analytically. First we expand the initial condition as a Fourier integral:

$$e^{-((y-y_a)/L)^2} = \sqrt{\pi}\frac{L}{2} \int_0^\infty e^{-k^2L^2/4} \cos(k(y-y_a))\, dk \tag{94}$$

Then, each mode evolves in time as:

$$e^{\sigma(k)\, t} \cos(k(y-y_a)) \tag{95}$$

with $\sigma(k) = -\epsilon\, k^2$, so that the solution will be:

$$x_s(y,t) = \sqrt{\pi}\frac{AL}{2} \int_0^\infty e^{-k^2L^2/4 - \epsilon k^2 t} \cos(k(y-y_a))\, dk \tag{96}$$

that can be cast into:

$$\begin{aligned} x_s(y,t) &= \frac{A}{\sqrt{1+4\epsilon t/L^2}} \frac{\sqrt{\pi}}{2} \sqrt{1+4\epsilon t/L^2} \int_0^\infty e^{-(k^2L^2/4)\sqrt{1+4\epsilon t/L^2}} \cos(k(y-y_a))\, dk \\ &= \frac{A}{\sqrt{1+4\epsilon t/L^2}}\, e^{-(y-y_a)^2/(L^2+4\epsilon t)} \end{aligned} \tag{97}$$

Therefore, $x_s(y_a, t) = A \,/\, \sqrt{1+4\epsilon t/L^2}$ and the diffusivity can be evaluated from:

$$\epsilon = \frac{L^2}{4t} \left(\frac{A^2}{x_s(y_a,t)^2} - 1 \right) \tag{98}$$

This expression allows for the computation of the effective coastline diffusivity when applied to the coastline position $x_s(y_a, t)$ predicted by the model. It will be also applied to the bed level $z_b(x_a, y_b, t)$ to compute the diffusivity experienced by the bathymetry and compare it with the coastline diffusivity. From the effective coastline diffusivity, ϵ, and eq. 93 the effective active depth for normal wave incidence

$$\bar{D} = 2\mu \frac{H_b^{5/2}}{\epsilon} \tag{99}$$

can be defined.

Figure 9 shows the time evolution of the bathymetry and the coastline during 50 days under normally incident regular waves of $H = 1$ m. The profile diffusivity coefficients are taken as $\epsilon_{xm} = 0.02, \epsilon_{ym} = 0.01$. It is seen that the shoal off the salient is eroded away and the sand is deposited offshore of both sides of it. This is very apparent at day 5. At the same time, the salient itself is eroded and smoothed. This process goes on and can also be seen at day 10. At day 15, the salient has been substantially reduced and the bathymetric lines become almost rectilinear. This tendency continues while slowing down and at day 50 both the coastline and the bathymetric lines are almost rectilinear as there were for the initial unperturbed coast. The time evolution of the tip of the salient, $x_s(y_a, t)$ is displayed in Figure 10. The analytical solution of eq. 92 with $\epsilon = 0.086$ m^{2}s^{-1} is also shown and it is found that it represents quite well the overall behaviour of the modelled coastline for the 50 days-period. Figure 5 shows a similar plot for $\epsilon_{xm} = 0.1, \epsilon_{ym} = 0.03$, where the analytical solution (has been assigned a diffusivity $\epsilon = 0.192 m^2 s^{-1}$. It is seen that in this case there is still a better agreement between model and analytical solution. The model therefore reproduces well the diffusive smoothing out of shoreline irregularities under normal incident waves. This diffusivity under these waves would correspond to an effective active depth of $\bar{D} = 3.5$ m which is very sensible in account that the depth of closure of the perturbation is $D_c = 5$ m.

5.1 Role of the profile diffusivity, ϵ_x, ϵ_y

Typically, there is in the model a delay between the surf zone morphodynamics and the coastline changes. This is apparent in Fig. 9 where a very significant erosion is seen offshore of the cusp at day 5 while the changes in the coastline position are still rather modest. This behaviour is still more apparent in Fig. 12 where the relative changes in coastline position, $(x_s(y_a, t) - \bar{x}_s)/(x_s(y_a, 0) - \bar{x}_s)$ are compared with the relative changes in bed level at a representative location in the surf zone, $(z_b(\bar{x}_s + X_b, y_a, t) - z_{be}(\bar{x}_s + X_b, y_a)/(z_b(\bar{x}_s + X_b, y_a, 0) - z_{be}(\bar{x}_s + X_b, y_a))$. It is clearly seen how the bed perturbation drops down very quickly to about 10 % of its initial value within a couple of days whereas the coastline perturbation decreases only to about a 90 % of its initial value. Afterwards, the bed level reverses its tendency and starts to oscillate. Interestingly, both relative changes tend to coincide as the system goes back to equilibrium as it is seen after day 40. This delay between surf zone bathymetric changes and shoreline position is desirable for modelling natural beach behaviour and is one of the capabilities of the new model which one line models can not account for.

The changes in the coefficients $\epsilon_{xm}, \epsilon_{ym}$ produce two effects: changes in the coast-

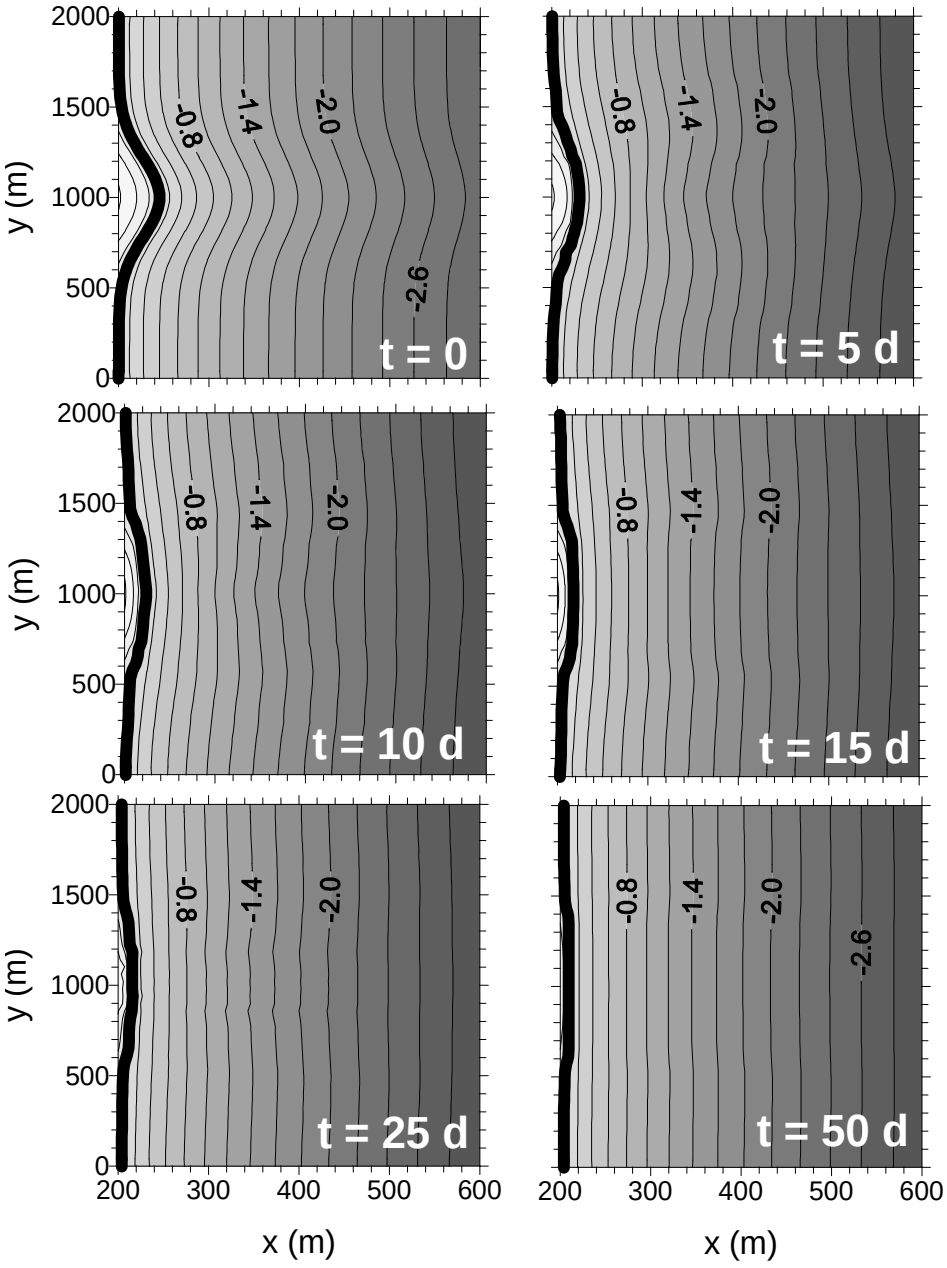

Figure 9: Time evolution of the coastline and the bathymetry in case of $\epsilon_{xm} = 0.02, \epsilon_{ym} = 0.01$, for waves of $H = 1$ m normally incident.

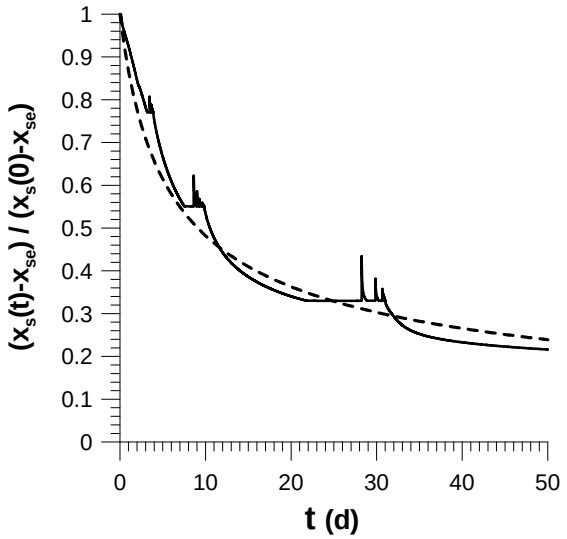

Figure 10: Modelled time evolution of the coastline, $x_s(y_a, t)$ (continuous line), and analytical solution of eq. 92 with $\epsilon = 0.086$ m^{2}s^{-1} (dashed line). Parameters as in Fig. 9.

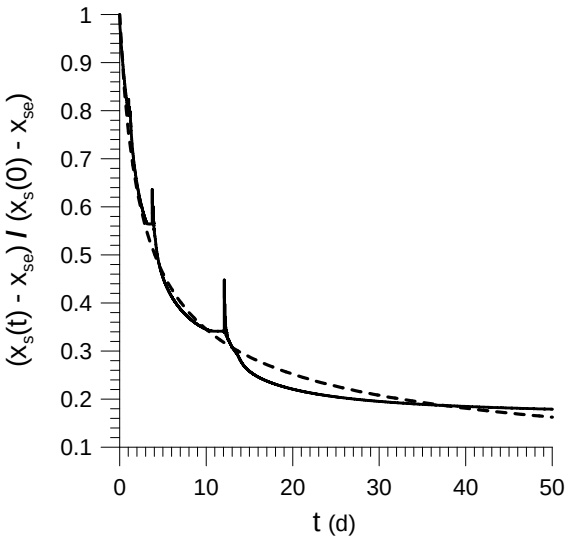

Figure 11: Relative time evolution of the shoreline at $y = 1000$ (continuous line) with $\epsilon_{xm} = 0.1, \epsilon_{ym} = 0.03$, versus analytic solution of eq. 92 for $\epsilon = 0.192 m^2 s^{-1}$(dashed line).

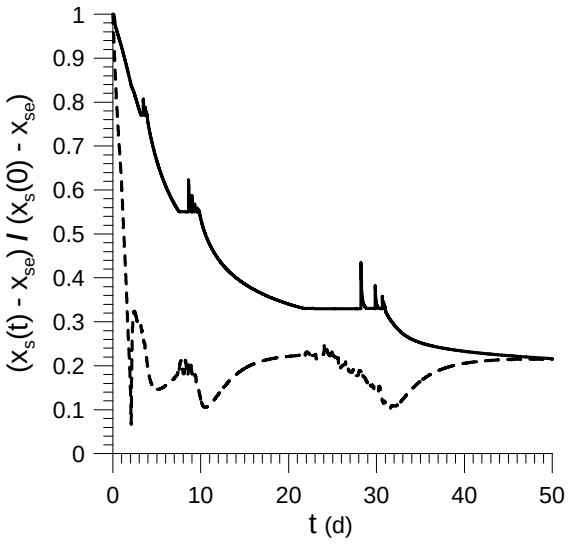

Figure 12: Relative time evolution of the shoreline at $y = y_a$ (continuous line) and of the bed level at $x = \bar{x} + X_b$, $y = y_a = 1000$ (dashed line). Parameters as in Fig. 9.

line diffusivity ϵ and changes in the delay between bathymetry and coastline. Values of ϵ_{xm} between 0.01 and 0.2 have been investigated with ϵ_{ym} typically a factor 2 to 3 smaller. The latter has been chosen for two reasons. First, the dynamics of the cross-shore profile is driven not only by turbulence but also by the organized wave-motion while the alongshore gradients are smoothed out only by the turbulence. Thus, it is expected that the tendency to equilibrium in the cross-shore direction will be faster than its alongshore counterpart. In addition, it seems advisable to keep the alongshore diffusivity as small as possible in order to avoid masking the diffusivity related to the wave-driven alongshore transport. As shown in Fig. 13, increasing ϵ_{xm} causes an increase in coastline diffusivity which tends to saturate for large values. If the profile diffusivity is too small, large gradients develop in the surf zone bathymetry and the model run eventually crashes. For instance, this occurred for $\epsilon_{xm} = 0.01, \epsilon_{ym} = 0.01$ and the bathymetry for day 2 is shown in Fig. 14.

The increase of ϵ_{xm} also causes a decrease on the delay between shoreline and bathymetry. As it is seen in Fig. 15 for $\epsilon_{xm} = 0.1$, $\epsilon_{ym} = 0.03$, for high values the shoreline reacts almost instantaneously to bathymetric changes.

The changes in the distances X_1, L cause changes in the diffusivity which are not very significant within the range of sensible values.

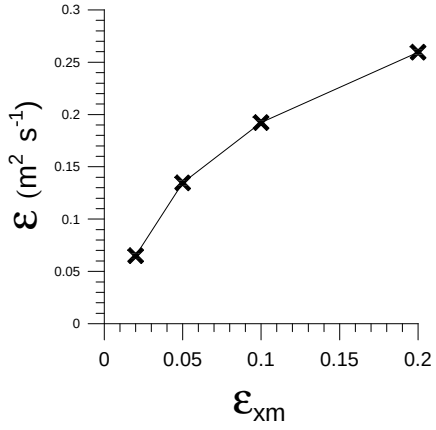

Figure 13: Coastline diffusivity ϵ as a function of profile diffusivity coefficient, ϵ_{xm}.

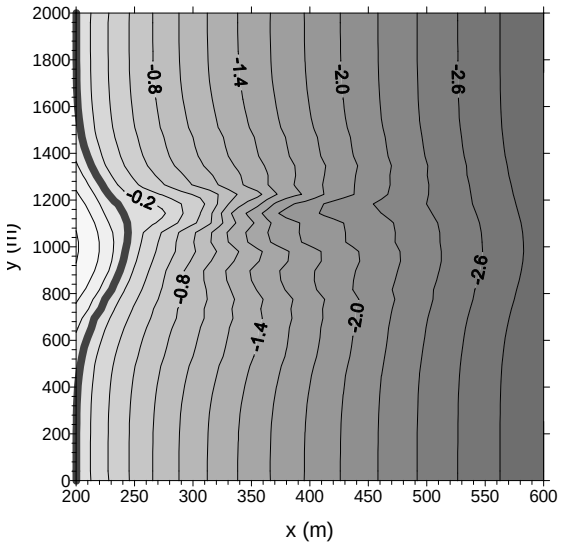

Figure 14: Shoreline and bathymetry for $t = 2$ days in case $\epsilon_{xm} = \epsilon_{ym} = 0.01$.

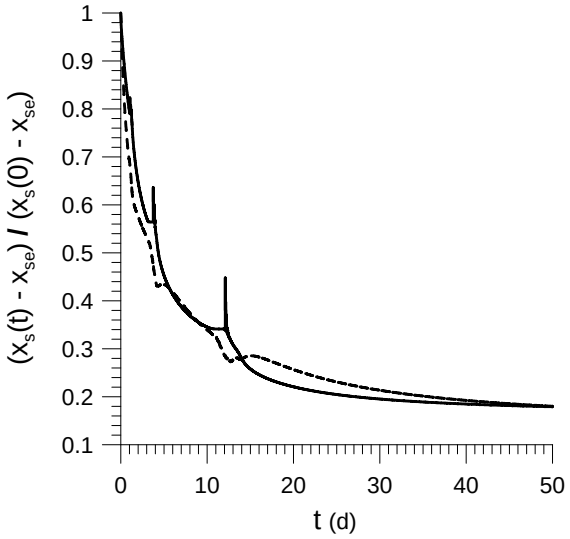

Figure 15: Relative time evolution of the shoreline at $y = y_a = 1000$ (continuous line) and of the bed level at $x = \bar{x}_s + X_b$, $y = y_a$ (dashed line), for $\epsilon_{xm} = 0.1$, $\epsilon_{ym} = 0.03$.

5.2 Role of the depth of closure of the perturbation

As shown in Fig. 16, increasing the depth of closure of the perturbation decreases the diffusivity, i.e., increases the active depth $\bar{D}$. This is obvious as more sand must be transported to come back to the equilibrium shoreline.

5.3 Dependence on the wave angle

Fig. 17 shows how the dependency of the diffusivity on wave angle in the model is roughly similar to the one predicted by the one line model, $\epsilon(\theta_b) = \epsilon(0)\cos(2\theta_b)$.

5.4 Dependence on the wave height

In view of eq. 93, one would expect that the shoreline diffusivity would increase with wave height as as power 2/5. However this is clearly not the case and it is puzzling since the active water depth in eq. 93 seems to be independent of the wave height. Indeed, according to the one line modelling [*Komar*, 1998; *Horikawa*, 1988; *Pelnard-Considère*, 1956], $\bar{D}$ is of the order of the depth of closure on that particular

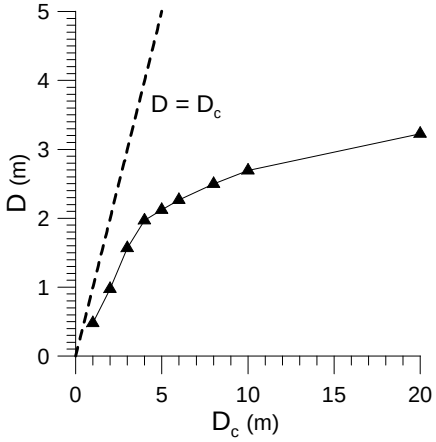

Figure 16: Averaged water depth, $\bar{D}$, as a function of the depth of closure of the bathymetric perturbation, D_c.

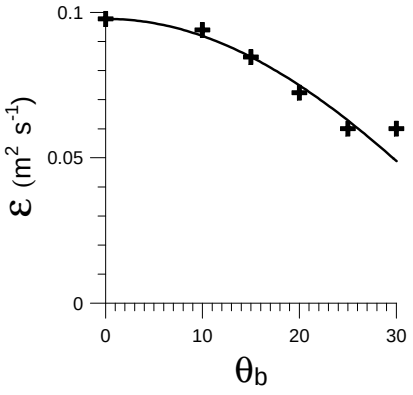

Figure 17: Coastline diffusivity as a function of wave angle at breaking (crosses). The continuous line represents $\epsilon(\theta_b) = \epsilon(0)\cos(2\theta_b)$

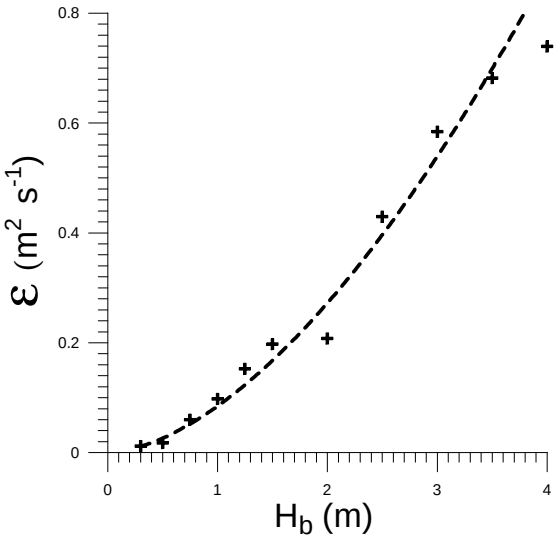

Figure 18: Coastline diffusivity as a function of wave height at breaking (crosses). The dashed line represents the best fit $\epsilon \simeq 0.085 H_b^{1.68}$.

coast which is related to the extreme storms in the wave climate. So, it does not depend on the instantaneous wave height. But that refers to a statistical run of the one line model in where the problem is: which is the shoreline evolution under a distribution of waves, for instance during one year, if one knows the mean annual wave height and the wave which is exceeded only 12 hours per year, H_e? Then if you keep H_e fix and you double the mean annual wave height the shoreline diffusivity would increase by a factor $2^{2/5}$. However, for a deterministic run with a fix wave height all the time, the active water depth should depend on this wave height. It is therefore reasonable that $\bar{D}$ depends on H_b for deterministic runs with fix wave height so that the dependence of the diffusivity on H_b is not the power 5/2 anymore.

It can be seen in Figs. 18 and 19 that ϵ is proportional to $H_b^{1.68}$ while $\bar{D}$ increases as $H_b^{0.82}$

Acknowledgments

This work is funded by the Ministerio de Ciencia y Tecnologia of Spain through the PUDEM project under contract REN2003-06637-C02-01/MAR

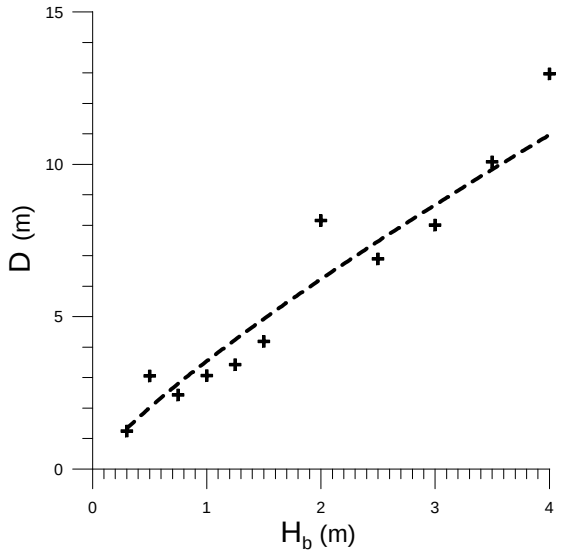

Figure 19: Effective active depth $\bar{D}$ as a function of wave height at breaking (crosses). The dashed line represents the best fit $\bar{D} \simeq 3.5 H_b^{0.82}$.

References

Ashton, A., A. B. Murray, and O. Arnault, Formation of coastline features by large-scale instabilities induced by high-angle waves, *Nature*, *414*, 296–300, 2001.

Caballeria, M., G. Coco, A. Falqués, and D. A. Huntley, Self-organization mechanisms for the formation of nearshore crescentic and transverse sand bars, *J. Fluid Mech.*, *465*, 379–410, 2002.

Falqués, A., Shoreline sand waves. Survey of available data., *Tech. rep.*, HUMOR project, Grup de Morfodinàmica de Costes, Appl. Physics Dept., Univ. Politècnica de Catalunya, Barcelona, Spain, 2002.

Falqués, A., On the diffusivity in coastline dynamics, *Geophys. Res. Lett.*, *30*(21), 2119, doi: 10.1029/2003GL017760, 2003.

Falqués, A., Wave driven alongshore sediment transport and stability of the Dutch coastline, *Coastal Eng.*, *53*, 243–254, 2005.

Falqués, A., and D. Calvete., Propagation of coastline sand waves, in *Proc. 3rd IAHR symposium on River, Coastal and Estuarine Morphodynamics,* vol. 2, edited by A. Sánchez-Arcilla and A. Bateman, pp. 903–912, Barcelona, Spain, 2003.

Falqués, A., and D. Calvete, Large scale dynamics of sandy coastlines. Diffusivity and instability, *J. Geophys. Res.*, *110*(C03007), doi:10.1029/2004JC002587, 2005.

Falqués, A., G. Coco, and D. A. Huntley, A mechanism for the generation of wave-driven rhythmic patterns in the surf zone, *J. Geophys. Res.*, *105*(C10), 24,071–24,088, 2000.

Falqués, A., N. Dodd, R. Garnier, F. Ribas, L. MacHardy, F. Sancho, P. Larroudé, and D. Calvete, Rhythmic surf zone bars and morphodynamic self-organization., *Coastal Eng.*, submitted, 2005.

Horikawa, K., *Nearshore Dynamics and Coastal Processes*, University of Tokio Press, Tokio, Japan, 1988.

Inman, D. L., Accretion and erosion waves on beaches, *Shore and Beach*, *55*(3/4), 61–66, 1987.

Komar, P. D., *Beach Processes and Sedimentation*, second ed., Prentice Hall, 1998.

Larson, M., and N. C. Kraus, Mathematical modeling of the fate of beach fill, *Coastal Eng.*, *16*, 83–114, 1991.

Larson, M., H. Hanson, and N. C. Kraus, Analytical solutions of the one-line model of shoreline change, *Tech. rep.*, US Army Corps of Engineers, 1987.

Pelnard-Considère, R., Essai de theorie de l'evolution des formes de rivage en plages de sable et de galets, in *4th Journees de l'Hydraulique, Les Energies de la Mer, Paris*, vol. III(1), pp. 289–298, Société Hydrotechnique de France, 1956.

Ribas, F., A. Falqués, and A. Montoto, Nearshore oblique sand bars, *J. Geophys. Res.*, *108*(C4), 3119, doi:10.1029/2001JC000,985, 2003.

Ruessink, B. G., and M. C. J. L. Jeuken, Dunefoot dynamics along the dutch coast, *Earth Surface Processes and Landforms*, *27*, 1043–1056, 2002.

Short, A. D., *Handbook of Beach and Shoreface Morphodynamics*, Wiley, Chichester, 1999.

Thevenot, M. M., and N. C. Kraus, Longshore sandwaves at Southampton Beach, New York: observations and numerical simulation of their movement, *Mar. Geology*, *126*, 249–269, 1995.